# EGUSphere-2024-665 – Response to referee 1

November 16, 2024

## 1 General comments from the referee

The manuscript "Viscoelastic mechanics of tidally induced lake drainage in the Amery grounding zone" by Zhang et al. explains the physics that drive a series of supraglacial lake drainage events in Antarctica with numerical models. Remote sensing data suggest that the extensional stress regime of the background ice flow is not enough to trigger the lake drainage events. They conduct a series of targeted numerical experiments to show that tidal flexure provides the necessary extensional stresses to drive hydrofracturing, depending on the depth of the supraglacial lake. This essentially confirms the hypothesis in the observational study [Trusel et al., 2022], that detailed these drainage events. While I have some comments primarily related to clarification and discussion, my judgment is that this would be an excellent contribution to TC.

We thank the reviewer for their constructive and insightful comments that have helped us improve the manuscript. Below we provide a detailed discussion of the comments and proposed changes. We use blue colour to indicate **comments**; our **replies** are in black.

## 2 Specific comments from the referee

In the last line of the abstract and conclusions you mention calving. While I understand that supraglacial lakes might play a role in ice-shelf breakup [Banwell et al., 2019], I was not exactly sure how the results in this study related to the calving front. Clearly there are similar physics because you are modelling fracture and flexure, but additional clarification would be helpful if you want to include this statement.

It was meant that the developed hydrofractures, if they remain open, can be advected downstream and destabilise the ice shelf by causing rifting. To avoid the confusion, we will remove the word "calving" and replace "rifting" with a general description "crevassing".

Introduction: Maxwell time of "approximately 9 hours in our estimation", this needs some more context for how you calculated this or a reference.

We will revise the paragraphs related to the Maxwell constitutive law. A detailed context for the revision can be found in the response to Referee 2. Below we provide details on how we choose the new set of rheological parameters and calculate the tidal stress.

Regularized flow law: It is good that you explicitly discuss the regularization because this is often not the case. I think it might be worth noting, with proper references, that the ice viscosity can vary over several orders of magnitude, and that the upper bound you have set seems to be on the lower end of the spectrum? Also suggest adding a statement here that you later test sensitivity to the Maxwell time.

We apologize for the typo related to the Maxwell time. The Maxwell time of ice in our model should be less than 40 hr instead of 9 hr. We recognise that the viscosity and Maxwell time are lower than their typical values. To address this, we will select the flow-law parameter $A_0 = 1.2 \times 10^{-25}$ Pa$^{-3}$ s$^{-1}$ with $n = 3$ at $T = -20$ °C in Glen's flow law [Cuffey and Paterson, 2010], as shown in Table 1. The modelled in-situ temperature at the lake region is between $-10$ °C and $-20$ °C [Wang et al., 2022], indicating that the real viscosity might be smaller. With these adjustments, the new Maxwell time is less than 5 d. In Figure 1 we provide results from a case with the new set of parameters. The tidal stress and grounding-line migration remain similar to the previous reference case, with only a slight change in magnitude.

Thanks for the constructive comment that helps us improve the model. A more detailed context about the rheology can be found in our response to Referee 2.

| Physical property | Notation | Value |
|---|---|---|
| Glen's Law exponent | $n$ | 3 |
| Viscosity coefficient | $A_0$ | $3.5 \times 10^{-25}$ Pa$^{-n}$ s$^{-1}$ |
| Shear modulus | $\mu$ | $0.30 \times 10^{9}$ Pa |
| Viscosity regularisation parameter | $\delta_\nu$ | $10^{-18}$ s$^{-2}$ |
| Upper bound of the viscosity | $2^{-(n+1)/2n} A_0^{-1/n} \delta_\nu^{-(n-1)/2n}$ | $1.2 \times 10^{14}$ Pa s |
| Maxwell time | $\tau$ | $\leq 5$ d |

Table 1: Rheological parameters used in numerical model and their reference values.

Section 2.1, last paragraph, "In B" should be "In Appendix B"?

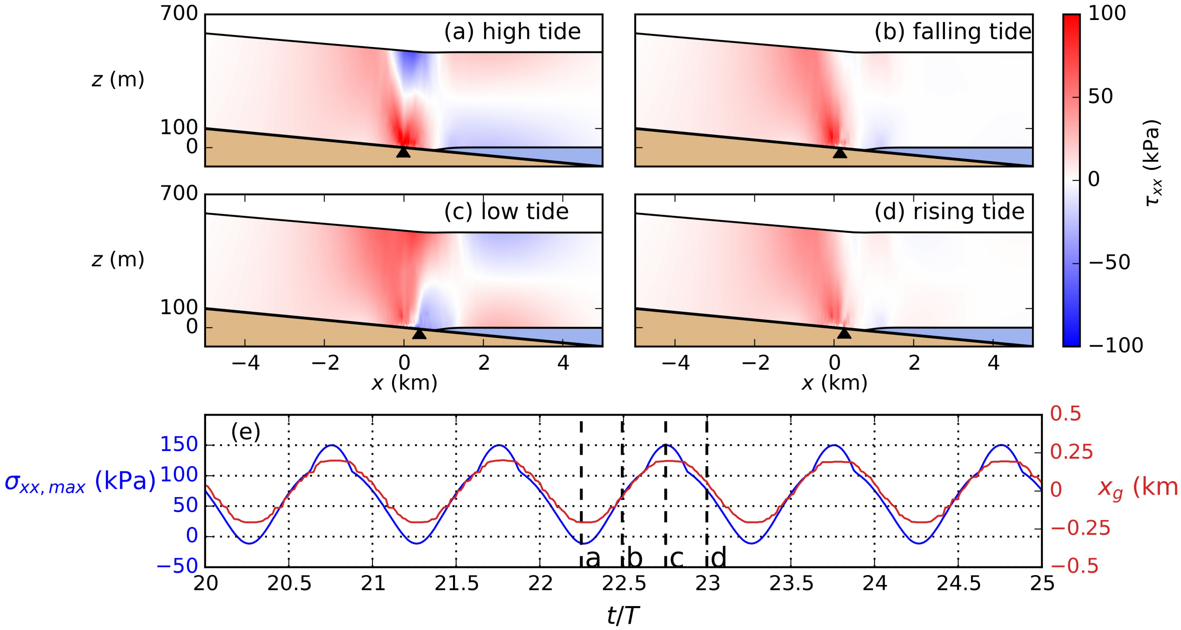


Figure 1: Tidal response of a marine ice sheet at different tidal phases, using the new set of parameters: $A_0 = 1.2 \times 10^{-25}$ Pa$^{-3}$ s$^{-1}$. **(a)–(d)** Deviatoric tensile stress $\tau_{xx}$ in one tidal period. **(e)** The maximum tensile stress $\sigma_{xx,max}$ (blue) on the top boundary within the lake region ($\bar{x_g} - 0.5$ km $\leq x \leq \bar{x_g} + 0.5$ km) and the GL position $x_g$ (red) versus time (scaled by the tidal period $T$) with positive values representing downstream migration. Vertical dashed lines show the time of panels (a)-(d).

Yes, we will change it.

When you introduce the upper-convected derivative, you should add a reference and probably provide some motivation (i.e. objectivity). The following review is excellent: Snoeijer J. H., Pandey A., Herrada M. A. and Eggers J. (2020). The relationship between viscoelasticity and elasticity. Proc. R. Soc. A. 47620200419

We will add the suggested reference and introduce the motivation to use the UCM model.

Comment somewhere on how the modelled grounding zone widths compare to width estimated from interferometry (Chen et al., 2023)?

Thanks for the suggestion for this model-data comparison. Chen et al. [2023] discussed the grounding zones of the feeding glaciers of the Amery Ice Shelf. Although the location is different from the lake position we have discussed, Chen et al. [2023] reported that near the grounding line with prograde bedslopes, the observed grounding-zone width is one order of magnitude larger than predicted from hydrostatic equilibrium that gives [Tsai and Gudmundsson, 2015]

$$\Delta x_g = \Delta h \left[ \beta + \frac{\rho_i}{\rho_w} (\alpha - \beta) \right]^{-1}, \tag{1}$$

where $\Delta h$ is the tidal range, $\alpha$ and $\beta$ are surface slopes and bed slopes along the flowline. In our reference case, the calculated grounding zone width $\Delta x_g \approx 500$ m is about 5 times the estimation from hydrostatic equilibrium (100 m). In our calculated width of the grounding zone, we neglect the effect of subglacial drainage system by assuming hydrostatic water pressure and rigid bedrock on basal ice.

After equation (18), "...variational formulation weakly converges...". To my knowledge, this is less obvious for the UCM model because it cannot be cast directly as a minimization problem like those dealt with in. Nevertheless, approximating the contact conditions by $\sigma_e = max\left(0, \sigma_e + \frac{1}{\varepsilon} u_n\right) \approx max\left(0, \frac{1}{\varepsilon} u_n\right)$, for small $\varepsilon$ (where $\sigma_e = \sigma_n - p_w$) still makes sense for UCM and motivates the use of a penalty term, as long as there aren't singularities in $\sigma_e$.

Thanks for raising this issue. We will state the difference between the viscous model and the UCM model, as well as the approximation used in the contact conditions.

Last paragraph of Section 2.5, "In A" should be "In Appendix A"?

Yes, we will change it.

Section 2.6 seems kind of random at first glance and needs more context... e.g., say what are you going to do later with the lake depths? Also, it might be better to place this after Section 2.1 rather than after the modelling material.

We will provide more context in Section 2.6 that gives our motivations for estimating lake depths in relation to the data-model comparison that follows. We will move this section up to follow Section 2.1.

Table 1: Units on viscosity and friction regularization parameters?

Units will be added.

Section 3.1: Specify that $\sigma - A$ relationship is for $\sigma_{xx,max}$.

When introducing the "$\sigma - A$ relationship", we will add a new sentence "Note that the '$\sigma$' here refers to the maximum tensile stress $\sigma_{xx,max}$ calculated above."

Figures 5 and 6 needs to label panels (a) and (b).

We will add panel labels.

Figure 5: clarify why the dashed lines go into the positive region? I thought they were compressive at high tide so not contributing to fracture, and I became confused.

Here the stress intensity factor depends on the vertical distribution of the net stress $\sigma_{xx}$ and the length of the fracture. On high tides, the bending stress is compressive on the top and tensile on the bottom. Meanwhile, the water pressure increases more quickly than the ice overburden stress with depth. If the fracture tip is located deeper in the ice, the propagation can be promoted by the water pressure, as well as the tensile bending stress in the lower part of the ice sheet.

Section 3.2: Not many details are provided about the weight function method. I presume that you are doing something with $\sigma_{xx,max}$, but some more context would be helpful.

We will add an appendix showing how we use the weight function method to calculate the stress intensity factor.

I don't think you say what is the value of fracture toughness $K_C$?

Thanks for pointing that out. We assume that the ice toughness $K_C = 100$ kPa m$^{1/2}$ [Rist et al., 1996], which is an estimate widely used in ice-fracture problems. We will add it to the table.

Section 3.3: All of this is in terms of the stress intensity factor, but I was wondering what are the stress thresholds associated with fracture propagation so that you can relate these to the background extensional stress ($<$ 40 kPa), which you say is not enough to cause fracture propagation on its own? Something to verify this claim would be good.

Thanks for raising this issue about demonstrating the LEFM model. We will rewrite the criterion in terms of the stress threshold and compare it with the observed background stress. In Fig. 6 of the manuscript, we have investigated the fracture propagation with the modelled background extensional stress when $A = 0$ m. The results suggest that with only the modelled background stress, the initial fracture will never propagate under any lake depth.

Section 3.3: "Supraglacial lakes would not be able to form under such large tidal stress." Does this limit correspond to the zero water depth in Figure 6 (state if so)? This is also an interesting point that you could revisit in the discussion.

Thanks for the constructive comment. Yes, this corresponds to the zero water depth where the criteria intercept the horizontal axis. In this case, the tidal stress is sufficiently large to induce crevassing without lake water supply, forming surface crevasses [Hulbe et al., 2016]. We will state this point explicitly and add a paragraph about this to the discussion.

Section 4: You are using present tense “We use” / “We construct” but you have already done these things at this point in the paper so maybe “We used” or “We have used”?

We will change it.

Section 4.1: Change “Ice Maxwell time” to “The Maxwell time of ice”?

We will change it. Thank you again for your helpful review.

# References


Alison F Banwell, Ian C Willis, Grant J Macdonald, Becky Goodsell, and Douglas R MacAyeal. Direct measurements of ice-shelf flexure caused by surface meltwater ponding and drainage. *Nature communications*, 10(1):730, 2019. doi: 10.1038/s41467-019-08522-5.

Hanning Chen, Eric Rignot, Bernd Scheuchl, and Shivani Ehrenfeucht. Grounding zone of amery ice shelf, antarctica, from differential synthetic-aperture radar interferometry. *Geophysical Research Letters*, 50(6):e2022GL102430, 2023. doi: 10.1029/2022GL102430.

Kurt M Cuffey and William Stanley Bryce Paterson. *The physics of glaciers*. Academic Press, 2010.

Christina L Hulbe, Marin Klinger, Megan Masterson, Ginny Catania, Kenneth Cruikshank, and Andrea Bugni. Tidal bending and strand cracks at the kamb ice stream grounding line, west antarctica. *Journal of Glaciology*, 62(235):816–824, 2016. doi: doi.org/10.1017/jog.2016.74.

MA Rist, PR Sammonds, SAF Murrell, PG Meredith, Hans Oerter, and CSM Doake. Experimental fracture and mechanical properties of Antarctic ice: preliminary results. *Annals of glaciology*, 23:284–292, 1996. doi: 10.3189/S0260305500013550.

Luke D Trusel, Zhuolai Pan, and Mahsa Moussavi. Repeated tidally induced hydrofracture of a supraglacial lake at the amery ice shelf grounding zone. *Geophysical Research Letters*, 49(7): e2021GL095661, 2022. doi: 10.1029/2021GL095661.

Victor C Tsai and G Hilmar Gudmundsson. An improved model for tidally modulated grounding-line migration. *Journal of Glaciology*, 61(226):216–222, 2015. doi: 10.3189/2015JoG14J152.

Yu Wang, Chen Zhao, Rupert Gladstone, Ben Galton-Fenzi, and Roland Warner. Thermal structure of the amery ice shelf from borehole observations and simulations. *The Cryosphere*, 16(4): 1221–1245, 2022.

# EGUSphere-2024-665 – Response to referee 2

November 16, 2024

We thank the reviewer for their constructive and insightful comments that have helped us improve the manuscript. Below we provide a detailed discussion of the comments and proposed changes. We use blue colour to indicate **comments**; our **replies** are in black.

## 1 Question on lateral shear

It shows that the flow of the outlet glacier is strongly affected by the lateral shear. The size of the arrows depicting the ice velocity are much lower outside of the centreline. My hand-drawn thin red line meant to illustrate how the along the flow ice-velocity component changes across the outlet glacier. This is a typical velocity profile of ice flow strongly affected by the lateral shear caused by the presence of the lateral confinement (e.g. Raymond, 1996 ). Its effects cannot be ignored. Consequently, they need to be accounted for either by having a three-dimensional model that includes the second horizontal dimension transverse to the ice flow and imposing the relevant conditions on the lateral boundaries, or by parameterizing them in the momentum balance eqn.(3). These effects of the lateral shear will substantially alter the model results.

Figure 1 (in this response) shows the velocity and strain rate within a 40 km × 20 km region centred at the lake, which is a zoomed-in version of Fig. 1 in our manuscript, using the modified rheological parameters (discussed below) of Table 1. We agree with the referee that the ice flow can be subject to lateral shear. However, the background ice-flow rate in this area is small, $\sim 20$ m/yr as shown in Figure 1(f). The transverse shear stress $|\tau_t| < 50$ kPa and along-flow extension $|\tau_p| < 100$ kPa in this region are smaller than the modelled tidal variations in Figure 2. That is why we have focused on tidally induced, along-flow extensional stress and have neglected the transverse shear when modeling tidal flexure. However, we acknowledge that this simplification could introduce error into the estimated background tensile stress at the grounding line, which in turn affects the fracturing criterion. We will discuss the limitation in our manuscript, and highlight this as an important direction for future research.

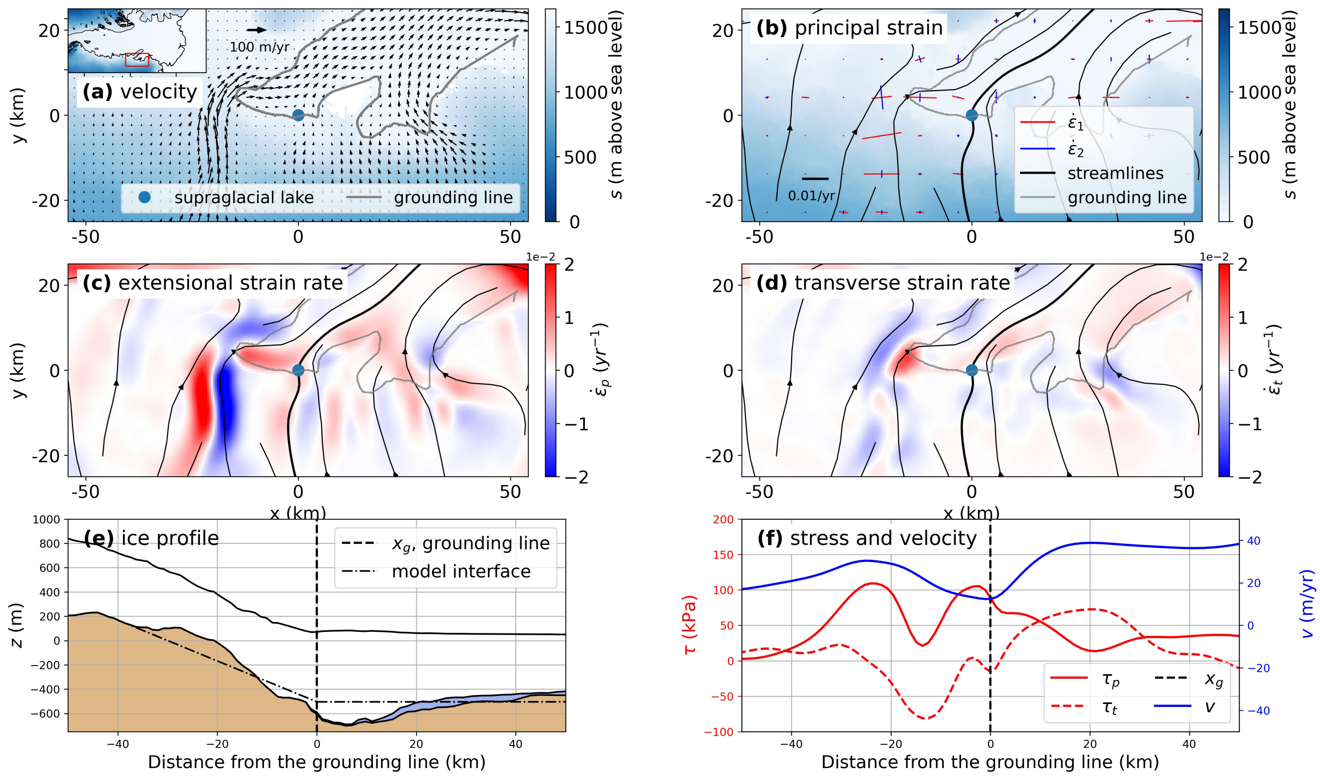


Figure 1: Ice surface velocity, strain rate and stress in the 40 km × 20 km region centred at the supraglacial lake, using the modified rheological parameters. **(a)** Velocity field near the grounding line (grey), where the supraglacial lake is denoted with the blue dot. The color represents the ice-sheet surface elevation above sea level. The map inset on the top left corner shows the full Amery Ice Shelf topography, with the plotted region outlined with a red box; **(b)** principal strain rate and streamlines. The streamline that crosses the lake is marked with the bold line; **(c)** along-flow strain rate; **(d)** transverse strain rate; **(e)** local ice-sheet geometry and bed topography; **(f)** For the streamline that crosses the lake, along-flow deviatoric extension $\sigma_p$ (solid red line) and shear stress $\sigma_t$ (dashed red line), and speed $v$ (blue). Note that $x = x_g = 0$ is the position of the supraglacial lake as well as the grounding line.

## 2 Question on ice rheology

Secondly, the quoted magnitude of the observed velocity imposed at the inflow boundary is low, 9 m/yr; so are the magnitudes of velocity shown in fig. 1f (a minor comment: it is unclear whether this velocity profile is computed or observed). Using parameters listed in table 1 and the Shallow Ice Approximation one could estimate the ice surface velocity resulted from the internal deformation only, assuming no-slip at the ice bed interface. That value is 20 m/yr, which is larger than the observed surface velocity by a factor of two. This suggests that (a) either the chosen parameters are off (specifically the ice stiffness parameter A0, which I will come back to) or (b) the ice flow is dominated, or strongly influenced, by the vertical shear, and the focus on the longitudinal stress $\tau_{xx}$ is unwarranted, or both.

Thank you for raising this issue with the background velocity. The 9 m/yr inflow velocity is the observed velocity averaged across the entire lake region from the MEaSUREs InSAR-Based Antarctica Ice Velocity Map [Rignot et al., 2016, Trusel et al., 2022]. We will make this clear by modifying the first sentence of section 2.1 in our manuscript.

On the flow line past the lake centre, the observed velocity is about 12 m/yr at the lake centre, and is about 17 m/yr at 10 km upstream of the lake centre. The estimate from Shallow Ice Approximation (20 m/yr) would better match the upstream surface velocity, instead of the lake region close to the grounding line. To improve the modelled background flow regime near the lake, instead of using the 9 m/yr velocity as the inflow velocity, we will use 17 m/yr at the inflow boundary in our model. We discuss the issue with ice viscosity in detail below.

Thirdly, the chosen value of A0 is very high. The ice-stiffness parameter is a function of the temperature of ice through its column. The chosen value would correspond to ice temperatures of the range from -5°C to -7°C, which is very warm. Although summer temperatures can exceed freezing point from time-to-time, as indicated by the supraglacial lakes, the annual mean surface temperature is around -20°C (e.g., Kittel et al., 2021). With ice flow primarily driven by the internal deformation, the ice temperature through the most of the ice column is not substantially warmer; it is only in the fairly narrow band near the bed it is warmer due to the geothermal heat flux. The very high chosen value of the ice stiffness parameter leads to a very low ice viscosity, of the order of $10^{13}$ Pa·s, which is at least an order, or more likely two orders of magnitude lower than the typical values of ice viscosity.

This brings me to the second problem with the study — the choice of the ice rheology. The authors have estimate it 9 hrs (the penultimate line on page 2) and 40 hrs (the penultimate line of section 2.3 page 6). For more realistic values of ice viscosity it is of the order 5–15 days, which is substantially longer than the period of diurnal tides that cause the ice flexure. This fairly unambiguously indicates that ice responds to diurnal tides as elastic medium. Two questions that immediately comes to mind — is it worth the effort the authors have gone through and complexity of the viscoelastic rheology? Can't one simulate it with much simpler elastic rheology?

| Physical property | Notation | Value |
|---|---|---|
| Glen's Law exponent | $n$ | 3 |
| Viscosity coefficient | $A_0$ | $1.2 \times 10^{-25}$ Pa$^{-n}$ s$^{-1}$ |
| Shear modulus | $\mu$ | $0.30 \times 10^{9}$ Pa |
| Viscosity regularisation parameter | $\delta_\nu$ | $10^{-18}$ s$^{-2}$ |
| Upper bound of the viscosity | $2^{-(n+1)/2n} A_0^{-1/n} \delta_\nu^{-(n-1)/2n}$ | $1.27 \times 10^{14}$ Pa s |
| Maxwell time | $\tau$ | $\leq 5$ d |

Table 1: Rheological parameters used in numerical model and their reference values.

We apologize for the typo related to the Maxwell time and thank the referee for pointing out this issue, which has helped us improve the model. The Maxwell time of ice in our model should be less than 40 hr instead of 9 hr. We recognise that the viscosity and Maxwell time are lower than their typical values. To address this, we will select the flow-law parameter $A_0 = 1.2 \times 10^{-25}$ Pa$^{-3}$ s$^{-1}$ with $n = 3$ at the temperature $T = -20$°C [Cuffey and Paterson, 2010] in Glen's flow law, as shown in Table 1. The modelled in-situ temperature at the lake region is between $-10$ °C and $-20$ °C [Wang et al., 2022]. With these adjustments, the new Maxwell time is less than 5 d. In Figure 2 we provide results from a case with the new set of parameters. The tidal stress and grounding-line migration remain similar to the previous reference case, with only an increase in magnitude.

In section 4.1, we discussed the effect of rheology on tidal stress by plotting the tidal stress $\sigma_{xx,\max}$ and grounding-zone width $\Delta x_g$ against the shear modulus $\mu$. These results are included here as Figure 3. The grounding-zone width and tidal stress decrease with ice becoming more elastic ($\mu \to 0$), indicating the sensitivity of the modelled tidal stress to ice rheology. Therefore, we considered the viscoelastic rheology to obtain an accurate estimate of the tidal stress.

Applying the new rheological parameter $A_0$ to the observations, the modified in-situ tensile stress near the lake is approximately 90 kPa (Figure 1), which is larger than the model's estimate (i.e., the time-average value of $\sigma_{xx,max} \sim 60$ kPa in Figure 2(e)). The $\sim$ 30-kPa discrepancy in the background stresses could arise from lateral stress or non-uniform ice properties. Although this discrepancy magnitude is smaller than the tidal stress, it could still introduce error into the model-based criterion. We will discuss these limitations in the manuscript to acknowledge potential sources of uncertainty in our model.

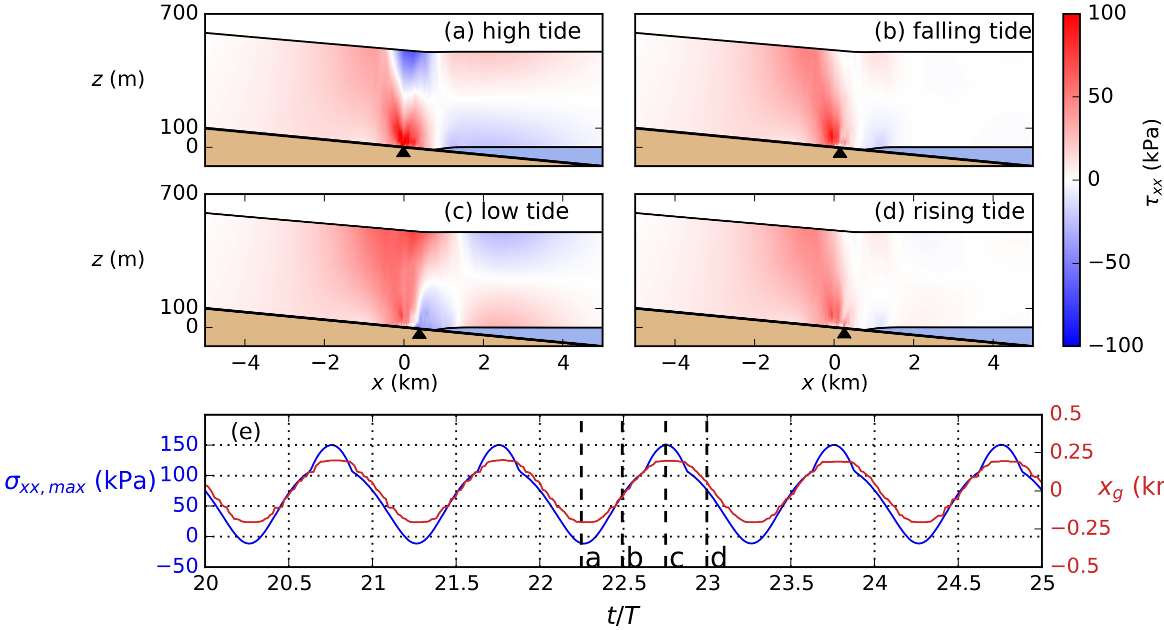


Figure 2: Tidal response of a marine ice sheet at different tidal phases, using the new set of parameters with $A_0 = 1.2 \times 10^{-25}$ Pa$^{-3}$ s$^{-1}$. **(a)–(d)** Deviatoric tensile stress $\tau_{xx}$ in one tidal period. **(e)** The maximum tensile stress $\sigma_{xx,max}$ (blue) on the top boundary within the lake region ($\bar{x_g} - 0.5$ km $\leq x \leq \bar{x_g} + 0.5$ km) and the GL position $x_g$ (red) versus time (scaled by the tidal period $T$) with positive values representing downstream migration. Vertical dashed lines show the time of panels (a)-(d).

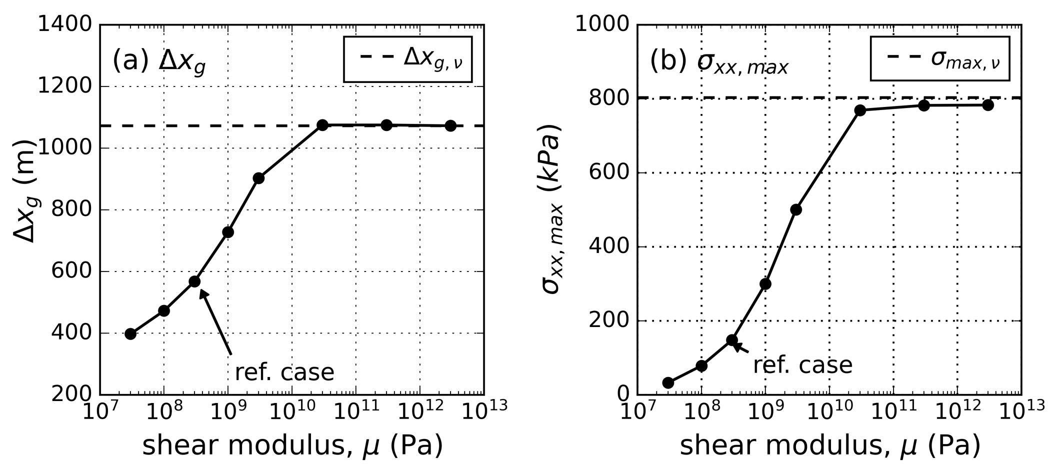


Figure 3: **(a)** The grounding-zone width $\Delta x_g$ (solid line), defined as $\Delta x_g = \max\{x_r\} - \min\{x_l\}$ as a function of shear modulus $\mu = 3 \times 10^7$ to $3 \times 10^{12}$ Pa, with $x_l$ and $x_r$ denote the left and right GL, respectively. The dashed line shows $\Delta x_{g,\nu}$, the grounding-zone width in the viscous limit ($\mu \to \infty$). **(b)** Maximum tensile stress $\sigma_{xx,max}$ versus $\mu$.

# References

Kurt M Cuffey and William Stanley Bryce Paterson. *The physics of glaciers*. Academic Press, 2010.

E Rignot, J Mouginot, and B. Scheuchl. Measures antarctic grounding line from differential satellite radar interferometry, version 2, 2016. URL https://nsidc.org/data/NSIDC-0498/versions/2.

Luke D Trusel, Zhuolai Pan, and Mahsa Moussavi. Repeated tidally induced hydrofracture of a supraglacial lake at the amery ice shelf grounding zone. *Geophysical Research Letters*, 49(7): e2021GL095661, 2022. doi: 10.1029/2021GL095661.

Yu Wang, Chen Zhao, Rupert Gladstone, Ben Galton-Fenzi, and Roland Warner. Thermal structure of the amery ice shelf from borehole observations and simulations. *The Cryosphere*, 16(4): 1221–1245, 2022.

# EGUSphere-2024-665 – Response to referee 3

November 16, 2024

We thank the reviewer for their constructive and insightful comments that have helped us improve the manuscript. Below we provide a detailed discussion of the comments and proposed changes. We use blue colour to indicate **comments**; our **replies** are in black.

## 1 Major comments

I found the information provided in section 3.2 about the LEFM model inadequate – I don't think sufficient information is provided to reproduce the stress intensity factors shown in the study.

Thank you for the constructive feedback. The LEFM model demonstrates the tidal and hydrostatic stress required to induce hydrofracturing from initial flaws with a given length. We have added an appendix C showing how we calculate the stress intensity factor with the weight function method.

Part of the stress field seen in figure 3 is a result of keeping the ice thickness fixed: In full-Stokes models, when you have flow across a slip/free slip boundary, the ice surface adjusts to have a very characteristic dip just downstream of the grounding line, which is a result of the speed up across this boundary (e.g., Barcilon and MacAyeal, 1993; Nowicki and Wingham, 2008). If the surface cannot adjust, residual stresses at the surface occur. Ideally, simulations would have been done with an evolving surface, but I understand that this is beyond the scope of this study. However, to account for this limitation, the difference of the deviatoric surface stress with tides and without (i.e., for a static grounding line) should be used (which I guess would be about 10 kPa less than the stresses shown, judging from the figures 3b and d).

Thanks for pointing out this limitation. In the model results in Figure 1 with revised rheological parameters, we found a background deviatoric tensile stress of approximately 30 kPa (Figure 1b,d), likely caused by the ice speed-up across the grounding line. The background stress will be extracted from the net stress in the fracture model. As the referee pointed out, our model does not fully capture the geometric complexities and background flow near the grounding line. We will include this limitation in our discussion.

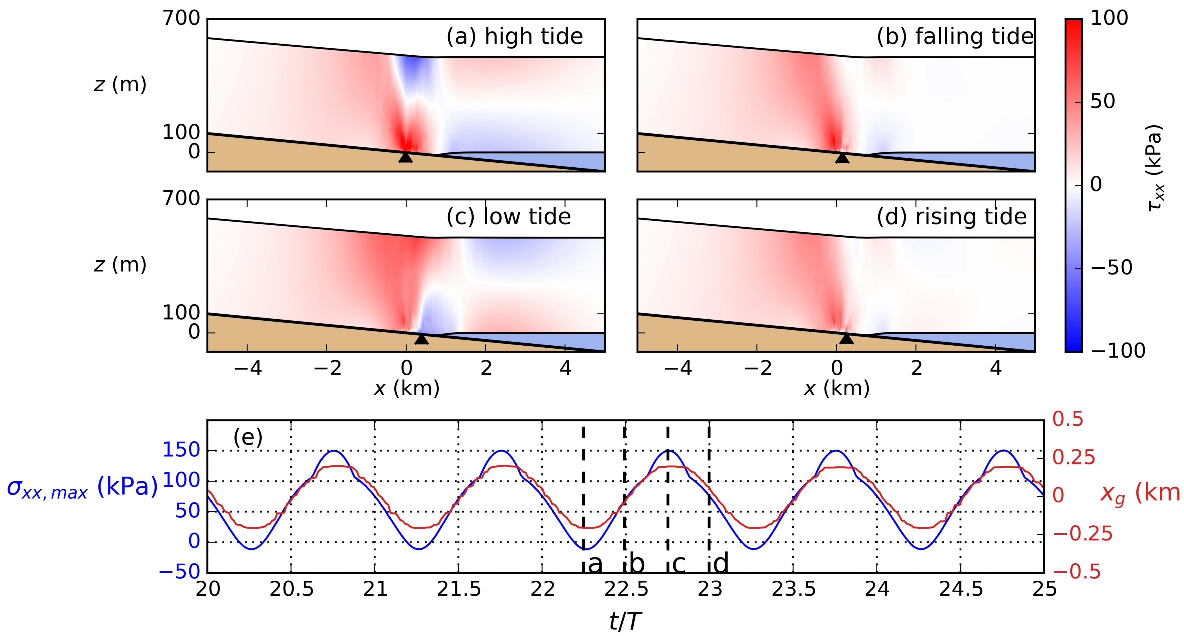


Figure 1: Tidal response of a marine ice sheet at different tidal phases, using the new set of parameters: $A_0 = 1.2 \times 10^{-25}$ Pa$^{-3}$ s$^{-1}$. **(a)–(d)** Deviatoric tensile stress $\tau_{xx}$ in one tidal period. **(e)** The maximum tensile stress $\sigma_{xx,max}$ (blue) on the top boundary within the lake region ($\bar{x_g} - 0.5$ km $\leq x \leq \bar{x_g} + 0.5$ km) and the GL position $x_g$ (red) versus time (scaled by the tidal period $T$) with positive values representing downstream migration. Vertical dashed lines show the time of panels (a)-(d).

The existence of a 10 m deep lake at the ice surface imposes a pressure of about 10 kPa at the ice surface, which is not necessarily negligible. How would that alter the stress considerations?

We agree with the referee that the supraglacial lake can modify the grounding-line migration, tidal stress, and hydrofracture propagation nearby. In the marine ice sheet model, the lake pressure can be accounted for by imposing an additional time-dependent lake pressure on the top of the ice sheet. During our initial model-development phase, we found that the influence of lake pressure on grounding-line dynamics is sensitive to the lake's position relative to the grounding line, since ice beneath the lake may shift from "grounded" to "floating" within one single tidal cycle. A supraglacial lake on a floating shelf can cause downward flexure [MacAyeal and Sergienko, 2013, Banwell et al., 2019, 2024], but this effect may be largely mitigated if the shelf regrounds on the bedrock during low tides. Additionally, the stress induced by the lake also depends on the specific geometry of the lake basin. While this is an intriguing topic, investigating the impact of the lake is beyond the scope of our current study. We believe future observations with higher-temporal-resolution data on lake depth and geometry near grounding lines could provide further insights into this process.

## 2 Minor comments

Page 4, 2nd line: "the the" → "the"

Will Change.

Page 4, 2nd paragraph: "The subglacial cavities downstream of the grounding zone are more than 20 m wide." I was confused by this, as BedMachine does not have 20 m resolution. What are you referring to here?

We apologise for the confusion. We are referring to the subglacial cavity being 20 m wide in the vertical. We stated this to show that the subglacial cavity under the floating shelf is large enough to allow free tidal oscillation without the formation of pinning points. Meanwhile, the water pressure can be approximated to be hydrostatic in the subglacial cavity. We will expand the sentence to include these details.

Figure 1b and caption: there is reference here to $\sigma_1$ and $\sigma_2$ but elsewhere in the text you refer to principle strain rates. Please make sure this is consistent.

We will modify the figure legend by using "principle strain rates" instead of "$\sigma_1$" and "$\sigma_2$".

Figure 6 and corresponding text: can you comment on the zero-tidal amplitude limit? Are the results what you would expect?

Thank you for the suggestion. The zero-tidal-amplitude limit represents a static grounding line with only the background tensile stress and the lake water pressure. It shows that without tides, the lake water pressure together with background stress is insufficient to drive hydrofracturing, even if the lake basin is filled with melt water ($d_w = 10$ m). This indicates that lake drainage only occurs with tides, thus is consistent with the hypothesis from Trusel et al. [2022].

## References


Alison F Banwell, Ian C Willis, Grant J Macdonald, Becky Goodsell, and Douglas R MacAyeal. Direct measurements of ice-shelf flexure caused by surface meltwater ponding and drainage. *Nature communications*, 10(1):730, 2019. doi: 10.1038/s41467-019-08522-5.

Alison F Banwell, Ian C Willis, Laura A Stevens, Rebecca L Dell, and Douglas R MacAyeal. Observed meltwater-induced flexure and fracture at a doline on george vi ice shelf, antarctica. *Journal of Glaciology*, pages 1–14, 2024. doi: 10.1017/jog.2024.31.

Douglas R. MacAyeal and Olga V. Sergienko. The flexural dynamics of melting ice shelves. *Annals of Glaciology*, 54(63):1–10, 2013. doi: 10.3189/2013AoG63A256.

Luke D Trusel, Zhuolai Pan, and Mahsa Moussavi. Repeated tidally induced hydrofracture of a supraglacial lake at the amery ice shelf grounding zone. *Geophysical Research Letters*, 49(7): e2021GL095661, 2022. doi: 10.1029/2021GL095661.